Tuning the Limiting Thickness of a Thin Oxide Layer on Al(111) with Oxygen Gas Pressure

Na Cai, Guangwen Zhou, Kathrin Müller, and David E. Starr

Phys. Rev. Lett. **107**, 035502 — Published 11 July 2011

DOI: 10.1103/PhysRevLett.107.035502

Tuning the limiting-thickness of a thin oxide layer on Al (111) with oxygen gas pressure

Na Cai, Guangwen Zhou*

Department of Mechanical Engineering & Multidisciplinary Program in Materials Science and Engineering, State University of New York, Binghamton, NY 13902

Kathrin Müller, David E. Starr

Center for Functional Nanomaterials, Brookhaven National Laboratory, Upton, NY 11973

Abstract

We report an x-ray photoelectron spectroscopy study of the oxidation of Al(111) surfaces at room temperature, which reveals that the limiting-thickness of an aluminum oxide film can be tuned using oxygen gas pressure. This behavior is attributed to a strong dependence of the kinetic potential on the oxygen gas pressure. The coverage of oxygen anions on the surface of the oxide film depends on the gas pressure leading to a pressure dependence of the kinetic potential. Our results indicate that a significantly large oxygen gas pressure (> 1 Torr) is required to develop the saturated surface coverage of oxygen ions, which results in the maximum kinetic potential and therefore the saturated limiting thickness of the oxide film.

* To whom correspondence should be addressed. E-mail: gzhou@binghamton.edu

Although oxide formation is favored thermodynamically for most metals and semiconductors, at low temperatures the reaction proceeds by an initial rapid oxidation stage followed by a drastic reduction of the oxidation rate to virtually zero. A generic model describing this limiting-thickness behavior of the oxide film growth kinetics is the Cabrera-Mott model [1, 2]. According to this model, an electric field is formed across the oxide film due to the potential difference of the metal/oxide work function and the oxygen/oxide work function resulting from electron tunneling between the Fermi level of the parent metal substrate and acceptor levels of chemisorbed oxygen at the surface. The self-generated electric field due to the potential difference of the metal/oxide work function and the oxygen/oxide work function (called the Mott Potential) reduces the energy barrier for the migration of ions through the oxide (the limiting step for mass transport in oxidation), leading to rapid initial oxidation rates at low temperature. As the tunneling current diminishes with increasing oxide film thickness, the oxidation virtually stops at a limiting-thickness.

Much recent research has been focused on influencing the self limiting process of low-temperature oxidation by manipulating the electric field assisted oxide growth. It has been shown that a significant impact on the oxidation kinetics can be achieved by either directly applying an external electric field [3-10] or electron bombardment of the oxide surface [11-13]. We demonstrate here that, the actual value of the self-generated electrostatic potential (designated as the kinetic potential [14]) can deviate from the Mott potential and is tunable by varying the oxygen gas pressure during oxidation which provides control of the limiting thickness of the oxide film. Our results indicate that a significantly large oxygen gas pressure is needed such that there is sufficient adsorbed oxygen at the oxide surface to accept the tunneling electrons in order to develop the maximum kinetic potential. At lower oxygen pressures, the lack of oxygen anions leads to a kinetic potential of lower magnitude and therefore a reduction in the limiting-thickness of the oxide film.

Our experiments were carried out in an ultrahigh vacuum (UHV) chamber equipped with an X-ray photoelectron spectrometer (XPS) – SPECS Phoibos 100 MCD analyzer, low-energy electron diffraction (LEED), and an Ar-ion sputtering gun. The chamber has a typical base pressure of 2×10^{-10} Torr. Al-Kα X-ray radiation (1486.7 eV) was used for the XPS studies. The Al(111) single crystal (1mm thick disk of 8 mm diameter) was purchased from Princeton Scientific Corp., cut to within 0.1° to the (111) crystallographic orientation and polished to a mirror finish. The sample was heated via a ceramic button heater. The temperature was measured with a type-K thermocouple. The crystal was cleaned by cycles of Ar^+ bombardment at 300K and annealing to 700 K. Surface cleanliness was checked with XPS. Oxygen gas (purity = 99.9999%) was introduced to the system through a variable pressure leak valve and the sample was oxidized at room temperature (300 K) under a controlled oxygen pressure, $p(O_2)$. For the initial stages of oxidation - oxygen coverages less than 1 monolayer where no attenuation of the Al peak was detectable, the oxide film thickness was measured with XPS by calculating the ratio of integrated O 1s and Al 2p core level peak intensities with atomic sensitivity factors (ASF) [15] that is correlated with the Al_2O_3 monolayer thickness (1 Al_2O_3 ML~ 0.2 nm) [16]. All the thicker continuous oxide films formed from the higher oxygen exposures (including longer time oxygen exposure at 1×10^{-8} Torr and the pressure from 1×10^{-8} Torr to 5 Torr) are determined using the attenuation of the metallic Al(2p) peak in the oxide films with the photoelectron attenuation length for Al_2O_3 (16.7± 0.6Å) [17, 18].

Fig. 1 shows the evolution of the oxide film thickness for Al(111) oxidation as a function of oxidation time for different oxygen gas pressures. The oxidation experiment starts with a clean Al surface which is oxidized first at $p(O_2) = 1\times10^{-8}$ Torr. The oxide film shows an initial fast growth stage followed by reduction in growth rate to the limited growth regime. Once no further changes in thickness are detected the oxygen pressure is increased. Each time after reaching a limiting oxide film thickness, a stepwise increase in oxygen pressure is applied and a thicker limiting oxide thickness is again observed after long time exposure. This shows that additional oxide growth is possible on oxide films with limiting

thicknesses established at lower pressure and that a new limiting thickness is observed in each pressure regime. This stepwise increase in the limiting-thickness of the oxide film continues (e.g. table 1) until an oxygen pressure of $p(O_2)$ ~ 1 Torr, beyond which the oxide film thickness remains essentially constant, irrespective of the prolonged oxygen exposure and further increase in oxygen pressure.

The above observations reveal that the limiting thickness of the oxide film increases with increasing oxygen gas pressure, despite the surface already being covered with an oxide layer with a limiting thickness at a lower oxygen pressure. To investigate if the pre-existing oxide film formed at the lower oxygen pressure has any effect on the subsequent oxide film growth at a higher oxygen pressure, we also examined the limiting-thickness of the oxide films formed by oxidizing clean Al surfaces at different oxygen pressures. As shown in Fig. 2, although the clean Al surfaces show a faster initial oxidation rate as compared to oxidation of the Al surfaces with a pre-existing oxide, they have nearly the same limiting oxide film thickness at a specific pressure as the oxide films formed by step-wise increases in pressure to this pressure. Their similar limiting thickness suggests that the self-limiting growth of the oxide film is determined by the oxygen gas pressure for a constant oxidation temperature.

The observed initially fast oxidation rate followed by a drastic reduction of the oxide film growth for each oxygen gas pressure is consistent with the Cabrera-Mott model of low temperature metal oxidation, which is characterized by the logarithmic growth law [1]

$$\frac{1}{X(t)} = A - B\ln t\,, \tag{1}$$

where X(t) is the thickness of the oxide film at the oxidation time t. For the mechanism that the oxide growth is limited by the ion migration under the electric field $E = -V_M/X(t)$ due to the Mott potential V_M, the coefficients A and B can be determined as [1, 19]

$$A = -\frac{kT}{qaV_M}\left[\ln\left(\frac{N\Omega qa\nu V_M}{kTX_L^2}\right) - \frac{U}{kT}\right], \quad \text{and} \quad B = -\frac{kT}{qaV_M}, \tag{2}$$

where N is the number density of oxygen ions on the surface, Ω is the volume of oxide formed per ion, q is the charge of the migrating ions, 2a is the distance between two adjacent potential minima, ν is the attempt frequency of the ion jump, k is the Boltzmann constant, T the temperature, X_L is the limiting thickness of the oxide film, and U denotes the diffusion barrier for the migration of ions.

By fitting the experimental data as shown in Fig. 1 to an inverse logarithm law for each oxygen gas pressure, the values of the Mott potential V_M and the rate-limiting energy barrier U for each oxygen gas pressure can be evaluated, provided that values for Ω, ν, q and a are known. The volume of oxide formed per Al cation, the attempt frequency of the Al cation jump, and the charge of the migrating Al cations can be taken equal to Ω=0.233 nm^3 [20, 21], $\nu=10^{12}\ s^{-1}$ [1, 21, 22], and q=3e (the elementary charge e = 1.6022×10^{-19} C) [21], respectively. For the oxidation of Al, the oxide films formed at low temperatures (T<200°C) are amorphous and can be described by a close packing of oxygen anions with the Al cations distributed over the octahedral and tetrahedral interstices and exhibit a deficiency of Al cations [21, 23]. This is indeed the case observed in our study. The stoichiometry of the oxide films formed with different oxygen gas pressures is approximately $Al_{(2-x)}O_3$ where x ~ 0.24, as determined from the Al/O peak intensity ratio. The rate-limiting energy barrier U for cation motion is associated with the hopping of Al cations between octahedral and/or tetrahedral interstices within the amorphous oxide film at low temperatures and the distance 2a between the nearest potential minima can be taken as 2a=2.4 Å for γ-Al_2O_3 [21, 23]. The obtained values of the Mott potential V_M and the activation energy barrier U for Al cation migration for the different oxygen gas pressures are given in Table 1.

For increasing oxygen pressures of 10^{-8}, 10^{-7}, 10^{-6}, 10^{-5}, 10^{-2}, and 1 Torr, we see in Table 1 that the Mott potential V_M increases from 0.066 V to 1.6 V. For $p(O_2)$ = 1 Torr and above, V_M saturates at a value of 1.6 V. We note that the rate-limiting diffusion energy barrier U is nearly constant at U = 1.54 eV for different oxygen pressures, suggesting that the nature of the defect structure in the amorphous

oxide films remains essentially unchanged under the different oxygen gas pressures. This is supported by their similar integrated Al/O peak intensity ratios of the oxide film formed with the different oxygen pressures. A recent study of oxide thin film growth for the oxidation of Al(111) has shown a lower value (~ 1eV) of the rate-limiting barrier for cation diffusion [24]. This deviation may be related to the different experimental techniques and procedures in the evaluation of the oxide film thickness, which result in the different values of the diffusion barrier.

The kinetic potential originates from the oxygen anion layer at the oxide surface and their Al cation counterparts at the metal-oxide interface. Previous results have demonstrated that when oxygen adsorbs onto an aluminum oxide thin film of fixed thickness on Al(111) at 80 K this electrostatic potential produces a shift of the Al-cation 2p core-level towards smaller binding energy (BE) relative to the metallic emission [25]. The metallic Al 2p core-level remains at constant BE because the Al substrate is at ground potential. We do not observe such a shift but instead have a nearly constant binding energy difference between the Al^{3+} and Al^{0} 2p peaks. This is likely due to competing effects arising from the different limiting oxide thickness at each new pressure. For example, previous studies of oxide thin films grown on metal substrates have demonstrated that the binding energies of both the cation and anion species shift towards higher binding energy and approach their bulk values as the oxide film increases in thickness [26, 27]. This has been attributed to a variety of metal – oxide interfacial effects including more effective screening of the core hole by the metallic substrate as well as band bending which decreases the core level binding energies when the oxide film is thin [28]. The influence of these effects on observed core level binding energies decreases as the oxide film thickens. The resulting increase in binding energy arising from a diminishing influence of these interfacial effects would work against the decrease in binding energy arising from the increase in the kinetic potential. This may cause the binding energy separation between the Al^{3+} and Al^{0} 2p peaks to be nearly constant in our study.

It is generally believed that the magnitude of the Mott potential is determined by the potential difference of the metal/oxide work function Φ_m and the oxygen/oxide work function Φ_o, i.e., $V_M = (\Phi_m - \Phi_o)/e$, where e is the elementary charge of electron. Since the work function is an intrinsic property, a tacit assumption made in the Cabrera-Mott oxidation model is that the Mott potential V_M is constant during the oxide growth, without considering the oxidation conditions [1]. This assumption is in contrast with the experimental results presented here, which reveal that this is true only if the oxygen gas pressure is sufficiently large. The actual electrostatic potential (i.e., the kinetic potential) created by the electronic species can be much smaller than the work function potential difference V_M for lower oxygen gas pressures.

To understand this pressure dependence of the kinetic potential at low oxygen pressures and determine at what conditions the maximum V_M can be developed, we calculated the equilibrium number density, N, of chemisorbed oxygen anions on the oxide surface under the various oxygen pressures. N is related to the Mott potential via $N = \frac{V_M \varepsilon_0 \kappa}{X_L e}$, as given by Gauss' theorem for a field between parallel plates [29], where ε_0 is electric constant in vacuum, κ is the relative permittivity and can be taken equal to κ= 9.6 [30], and X_L is the limiting thickness. The values for the number density N and therefore the surface coverage, Θ, (using the density of Al in the Al(111) surface as the reference surface) of adsorbed oxygen ions for different oxygen gas pressures are determined and given in Fig. 3(b). It can be seen that the calculated oxygen anion surface coverage increases with increasing the oxygen pressure and becomes saturated at the oxygen pressure of 1 Torr and above.

According to the Langmuir isotherm for dissociative gas adsorption, the dependence of the equilibrium oxygen anion coverage on the oxygen gas pressure $p(O_2)$ is given by $\Theta = \frac{\sqrt{b\mathbf{p}(\mathbf{O}_2)}}{1+\sqrt{b\mathbf{p}(\mathbf{O}_2)}}$, where b is a constant which depends on temperature only [31]. We use the Langmuir isotherm to fit the

determined oxygen anion coverage and get an estimate of at which pressure the oxygen anion concentration saturates leading to the largest kinetic potential. As shown in Fig. 3, the maximum oxygen surface coverage is reached for oxygen pressure beyond ~ 1 Torr, which is close to our observed experimental pressure required for the maximum kinetic potential. Since the amount of adsorbed oxygen that can be ionized by tunneling electrons is less at a lower oxygen gas pressure, a corresponding lower magnitude of the electric potential is developed across the oxide layer. As shown in Fig. 3, a very large oxygen pressure (i.e., $p(O_2)$ = 1 Torr) is needed in order to develop a full oxygen surface coverage that provides a sufficient amount of adsorbed oxygen at the oxide surface to accept the tunneling electrons. As a result, the maximum Mott potential can be developed at these higher oxygen gas pressures leading to the largest limiting thickness of the oxide film.

In summary, we have studied the limiting-thickness of the Al_2O_3 film formed during oxidation of an Al(111) surface with more than 9 orders of magnitude in oxygen pressure difference (10^{-8} - 5 Torr). We observe that the limiting-thickness of the oxide film increases with increasing the oxygen gas pressure to a pressure of about 1 Torr, beyond which the limiting thickness becomes saturated at ~ 12.4 Å. The obtained values of the kinetic potential and oxygen surface coverage reveal that a significantly large oxygen gas pressure is needed to provide the maximum coverage of oxygen anions on the oxidized surface, which results in the maximum kinetic potential within the oxide film. Such strong oxygen-pressure dependence of the generated electric field on the oxide growth has been hitherto rarely addressed, but may be crucial for understanding the difference in the response of a metal surface exposed to the conventional high vacuum environment typically employed in surface science related studies and the technologically relevant (at or near) atmospheric oxidation.

Acknowledgement: We acknowledge support from the National Science Foundation Grant No. CBET-0932814 and the Department of Energy Grant No. DE-FG02-09ER46600. Research carried out in part at

the Center for Functional Nanomaterials, Brookhaven National Laboratory, which is supported by the U.S. Department of Energy, Office of Basic Energy Sciences, under Contract No. DE-AC02-98CH10886.

References:

1 N. Cabrera and N. F. Mott, Rep. Prog. Phys. **12**, 163 (1949).

2 A. T. Fromhold, Jr., *Fundamental Theory of Metal Oxidation* (North-Holland Publishing Company, Amsterdam, 1976).

3 A. E. Gordon, R. T. Fayfield, D. D. Litfin, and T. K. Higman, J. Vac. Sci. Technol. B **13**, 2805 (1995).

4 C. Nowak, R. Kirchheim, and G. Schmitz, Appl. Phys. Lett. **89**, 143104 (2006).

5 P. Avouris, T. Hertel, and R. Martel, Appl. Phys. Lett. **71**, 285 (1997).

6 H. Kuramochi, K. Ando, T. Tokizaki, and H. Yokoyama, Appl. Phys. Lett. **84**, 4005 (2004).

7 C. Nowak, G. Schmitz, and R. Kirchheim, Surf. Sci. **604**, 641 (2010).

8 S. K. R. S. Sankaranarayanan, E. Kaxiras, and S. Ramanathan, Energy & Environmental Science **2**, 1196 (2009).

9 S. K. R. S. Sankaranarayanan and S. Ramanathan, J. Phys. Chem. C **114**, 6631 (2010).

10 S. K. R. S. Sankaranarayanan, E. Kaxiras, and S. Ramanathan, Phys. Rev. Lett. **102**, 095504 (2009).

11 I. Popova, V. Zhukov, and J. T. Yates, Jr., Phys. Rev. Lett. **89**, 276101 (2002).

12 V. Zhukov, I. Popova, and J. T. Yates, Jr., Phys. Rev. B **65**, 195409 (2002).

13 H. D. Ebinger and J. T. Yates, Jr., Phys. Rev. B **57**, 1976 (1998).

14 A. T. Fromhold, Jr. and E. L. Cook, Phys. Rev. B **163**, 650 (1967).

15 C. D. Wagner, L. E. Davis, M. V. Zeller, J. A. Taylor, R. H. Raymond, and L. H. Gale, Surf. Interface Anal. **3**, 211 (1981).

16 L. P. H. Jeurgens, W. G. Sloof, F. D. Tichelaar, and E. J. Mittemeijer, Phys. Rev. B. **62**, 4707 (2000).

17 H. Graupner, L. Hammer, K. Heinz, and D. M. Zehner, Surf. Sci. **380**, 335 (1997).

18 F. L. Battye, J. G. Jenkin, J. Liesegang, and R. C. G. Leckey, Phys. Rev. B **9**, 2887 (1974).

19 L. P. H. Jeurgens, W. G. Sloof, F. D. Tichelaar, and E. J. Mittemeijer, J. Appl. Phys. **92**, 1649 (2002).

20 E. Fromm, *Kinetics of Metal-Gas Interactions at Low Temperatures: Hydriding, Oxidation, Poisoning* (Springer, Berlin, 1998).

21 L. P. H. Jeurgens, W. G. Sloof, F. D. Tichelaar, and E. J. Mittemeijer, Phys. Rev. B. 62, 4707 (2000); J. Appl. Phys. 92, 1649 (2002); Surf. Sci. 506, 313 (2002); Thin Solid Films 418, 89 (2002).

22 P. C. J. Graat, M. A. J. Somers, A. M. Vredenberg, and E. J. Mittemeijer, J. Appl. Phys. **82**, 1416 (1997).

23 P. C. Snijders, L. P. H. Jeurgens, and W. G. Sloof, Surf. Sci. **496**, 97 (2002).

24 F. Reichel, L. P. H. Jeurgens, and E. J. Mittemeijer, Acta Materialia **56**, 2897 (2008).

25 C. Ocal, S. Ferrer, and N. Garcia, Surf. Sci. 163, 335 (1985).

26 S. Altieri, L. H. Tjeng, F. C. Voogt, T. Hibma, and G. A. Sawatzky, Phys. Rev. B 59, R2517 (1999).

27 D. E. Starr, F. M. T. Mendes, J. Middeke, R.-P. Blum, H. Niehaus, D. Lahav, S. Giumond, U. A., T. Kluener, M. Schmal, H. Kuhlenbeck, S. Shaikhutdinov, and H.-J. Freund, Surf. Sci. 599, 14 (2005).

28 C. Noguera, Physics and Chemistry at Oxide Surfaces (Cambridge Univeristy Press, Cambridge, UK, 1996).

29 F. P. Fehlner, Low-Temperature Oxidation (John Wiley & Sons, Inc., New York, 1986).

30 K. S. Shamala, L. C. S. Murthy, and K. N. Rao, Materials Science and Engineering B-Solid State Materials for Advanced Technology 106, 269 (2004).

31 K. Christmann, Introduction to Surface Physical Chemistry (Springer, New York, 1991).

Table caption:

Table 1: Limiting thickness of the oxide films, values of kinetic potential V_M, rate-limiting energy barrier U for cation motion, and oxygen coverage calculated from the oxygen uptake curves under different oxygen gas pressures.

Pressure (Torr)	1×10^{-8}	1×10^{-7}	1×10^{-6}	1×10^{-5}	1×10^{-2}	1	5
Limiting oxide thickness (Å)	2.42	3.81	5.14	5.99	11.30	12.42	12.43
Kinetic potential V_M (V)	0.066	0.137	0.341	0.664	1.026	1.620	1.620
Rate-limiting energy barrier U (eV)	1.534	1.550	1.534	1.540	1.536	1.546	1.546
Oxygen coverage (Θ)	0.031	0.058	0.126	0.306	0.516	0.963	0.963

Figure captions:

Figure 1

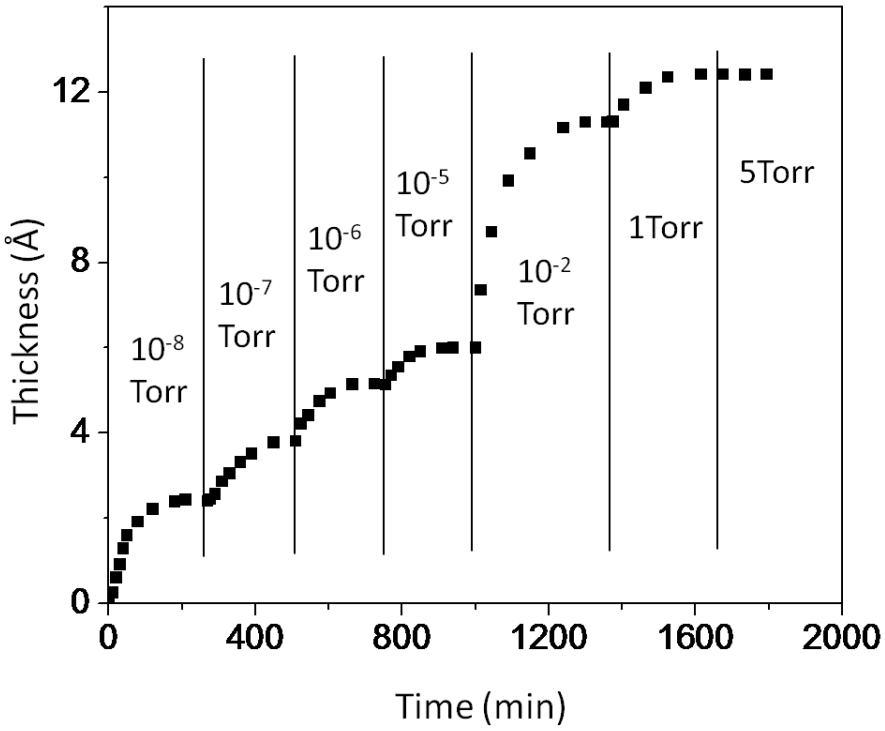

Fig. 1: Oxide film thickness as a function of oxidation time and oxygen gas pressure. The oxidation starts with a clean Al(111) surface which is oxidized first at $p(O_2) = 1\times10^{-8}$ Torr. A stepwise increase in oxygen pressure is applied after a limiting oxide thickness is reached at each oxygen pressure. The stepwise increase in oxygen pressure results in a corresponding increase of the limiting-thickness of the oxide film until an oxygen pressure of $p(O_2) = 1$ Torr is reached, beyond which the additional oxygen exposure to the surface does not result in any subsequent oxide growth.

Figure 2:

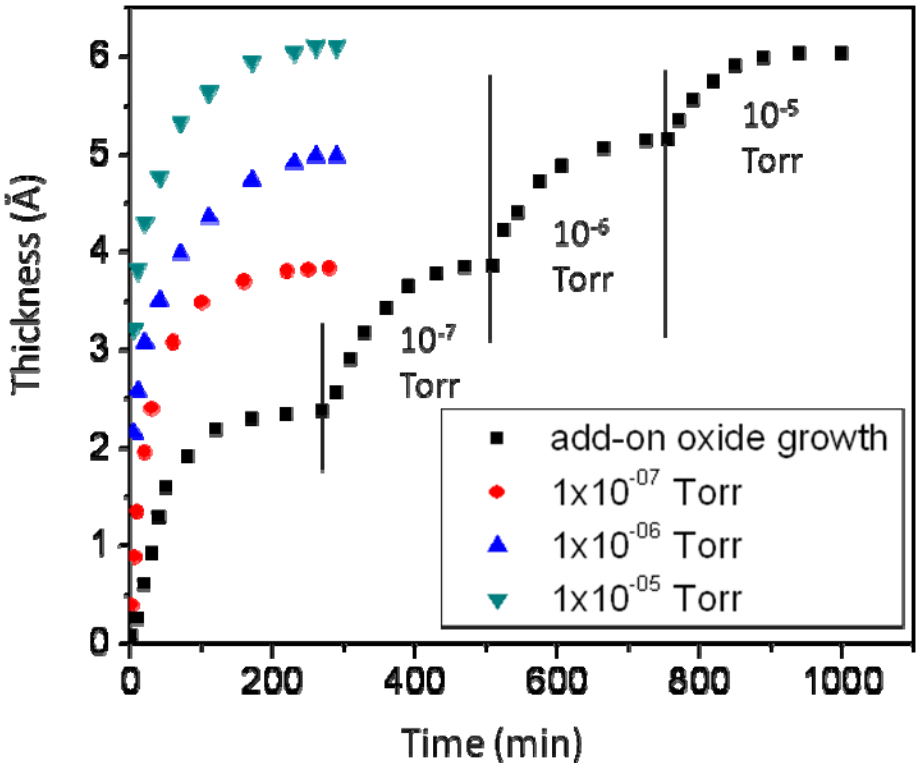

Fig. 2: Comparison of the oxidation kinetics of a freshly cleaned Al(111) surface to that of an Al(111) surface oxidized by step-wise increases in oxygen pressure. Both give a similar limiting-thickness of the oxide films at the same oxygen gas pressure, irrespective of whether the surface is covered with a pre-existing oxide layer formed at a lower oxygen pressure or not.

Figure 3:

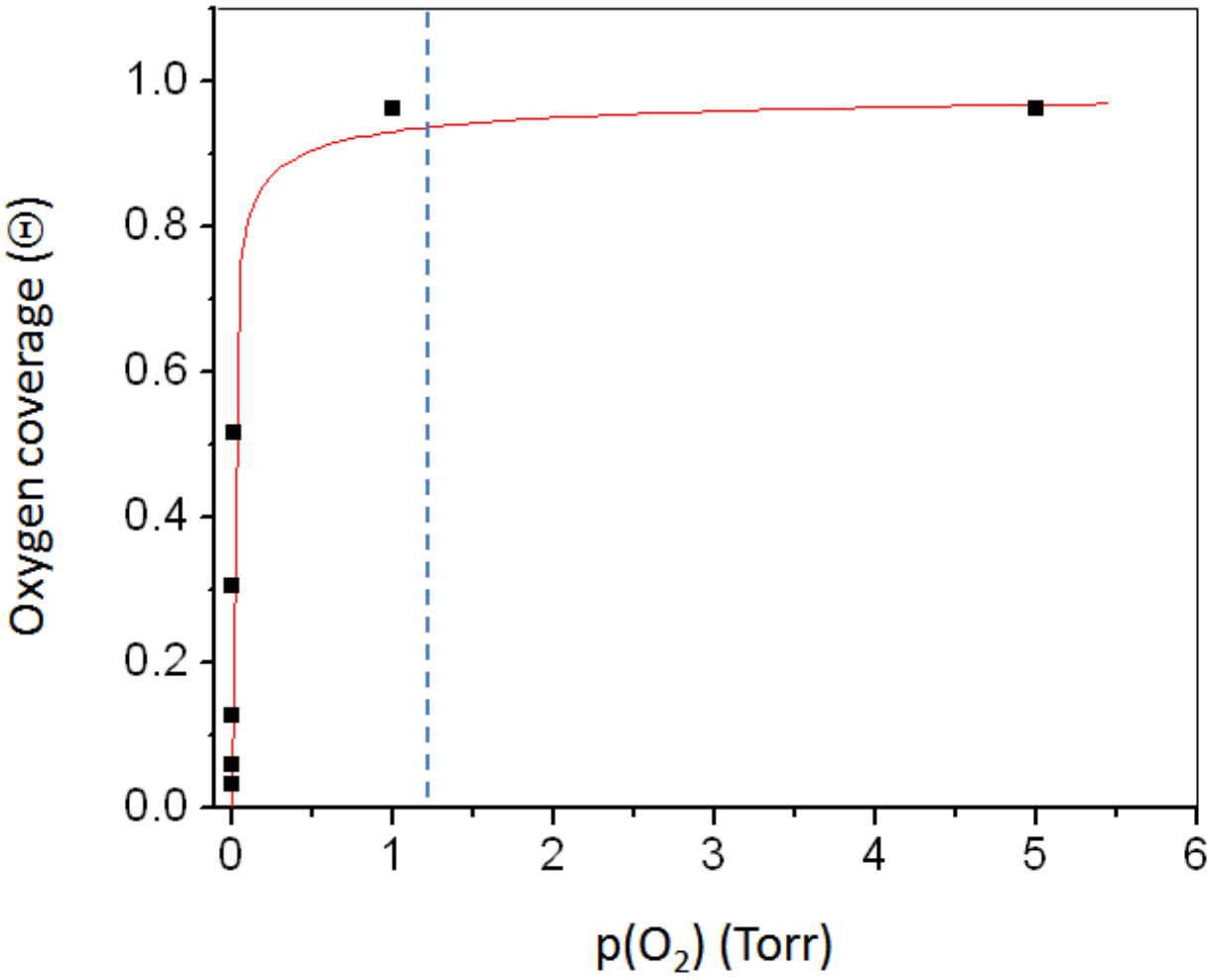

Fig. 3: Equilibrium surface coverage of oxygen ions with respect to the oxygen gas pressure. The solid line corresponds to a theoretical fitting to the Langmuir isotherm for dissociative oxygen adsorption. The dashed line indicates the approximate oxygen pressure beyond which the maximum oxygen surface coverage is reached.